A Self-powered Extensible SECE Rectifier For Piezoelectric Energy Harvesting

Jiacong Qiu, Junrui Liang
School of Information Science and Technology, ShanghaiTech University, Shanghai, China
*E-mail: {qiujc, liangjr}@shanghaitech.edu.cn

***Abstract*—Harvesting vibration energy from the environment using piezoelectric energy harvesters (PEHs) helps achieve battery-free embedded devices. Synchronous electric charge extraction (SECE) has load-independent power output. It is suitable for harvesting energy from multiple piezoelectric transducers. This paper presents a self-powered SECE interface circuit for piezoelectric energy harvesting. The proposed interface circuit implements a passive zero-crossing detection, harvests energy from multiple piezoelectric transducers with only one inductor, and outputs 79.3% more power than a standard full bridge rectifier in experiment.**

Keywords—piezoelectric energy harvesting (PEH), self-powered, synchronized electric charge extraction(SECE)

I. Introduction

Over the years, vibration energy harvesting has been a popular research topic. Vibration energy is widely available in ambient environment and can be used to power embedded systems like wireless sensor nodes. These devices may become self-powered and even get rid of batteries by using vibration energy[1].

In vibration energy harvesting using piezoelectric materials, different interface circuits have been proposed. A simple and direct approach is to use a full bridge rectifier. (FBR). It is also known as the standard energy harvesting (SEH) circuit.

For weakly coupled piezoelectric energy harvesters (PEHs), many interface circuits based on synchronized switch were proposed to improve the harvesting capability. The first synchronized switch technique was proposed in [2] and is known as parallel synchronized switch harvesting on inductor (P-SSHI). Another kind of harvesting technique is synchronous electric charge extraction (SECE) [3]. The self-powered versions of these interface circuits were also proposed to eliminate the need of extra sensors and external power supplies [4].

To harvest more energy, the possibilities of using multiple harvesters to form a PEH array were explored [5][6][7][8][9]. PEH arrays can harvest energy at a wider range of frequencies or from different directions. The vibration amplitudes and frequencies are usually different.

Multiple PEHs in an PEH array can share the inductor and output capacitor. Sharing components helps reduce cost and volume of the system. Ref. [4] presents a self-powered SECE circuit with shared zero-crossing detector for PEH voltage. Active components are used to achieve precise switching control and low conduction loss. [10] presents a SECE interface circuit with passive components and utilizes envelope detection to achieve peak detection. Although the peak output power of SECE is only a half of that of P-SSHI scheme [11], SECE is still an excellent candidate for array harvesting. Since the power output is load-independent, it can handle multiple PEHs with different electromechanical characteristics.

A self-powered SECE circuit for piezoelectric energy harvesting arrays with passive zero crossing detection (ZSECE) is developed. This circuit can harvest energy from multiple PEHs regardless of their phase differences. Its input voltage can be as high as 16 V peak-to-peak. Precise peak detection is achieved using a comparator. Passive zero-crossing detection scheme is implemented to reduce the cost of the circuit by eliminating the need for another comparator and logic gate, compared with the active zero-crossing detection scheme in [4]. No extra cold-start circuitry is needed. The circuit only needs off-the-shelf components to build.

II. ZSECE Interface Circuit

Fig. 1 shows the schematic of ZSECE circuit. It comprises five modules: a full-wave rectifier, a pre-harvesting module, a peak detector, and SECE interface with zero-crossing detection. L, D4 and C_{load} in the SECE interface can be shared by multiple PEHs.

A. Operation Principle of SECE Interface Circuit

Fig. 2 shows a general SECE circuit. It is a typical harvesting scheme based on synchronized switch technique. At the voltage peaks of PEH, the switch S is turned on. The inductor and parasitic capacitor of the PEH together forms a resonant loop. The energy stored in the parasitic capacitor C_p is transferred to the inductor. Fig. 3 shows the harvester voltage v and inductor current i_L waveform of SECE circuit. In ideal case, the switch will be turned off after all the energy has been transferred to the inductor, which is also the time when the voltage across the parasitic capacitor reaches 0. After the switch has been turned off, the current in the inductor will be freewheeled to the load.

To harvest energy from multiple PEHs, the circuit can be extended as shown in Fig. 4. Since the inductor only conduct current in one direction, multiple inductors can harvest energy at the same time without interfering one another, even if their phase difference is comparable to $(t_0 - t_1)$ [12]. The circuit can be extended further in the same manner.

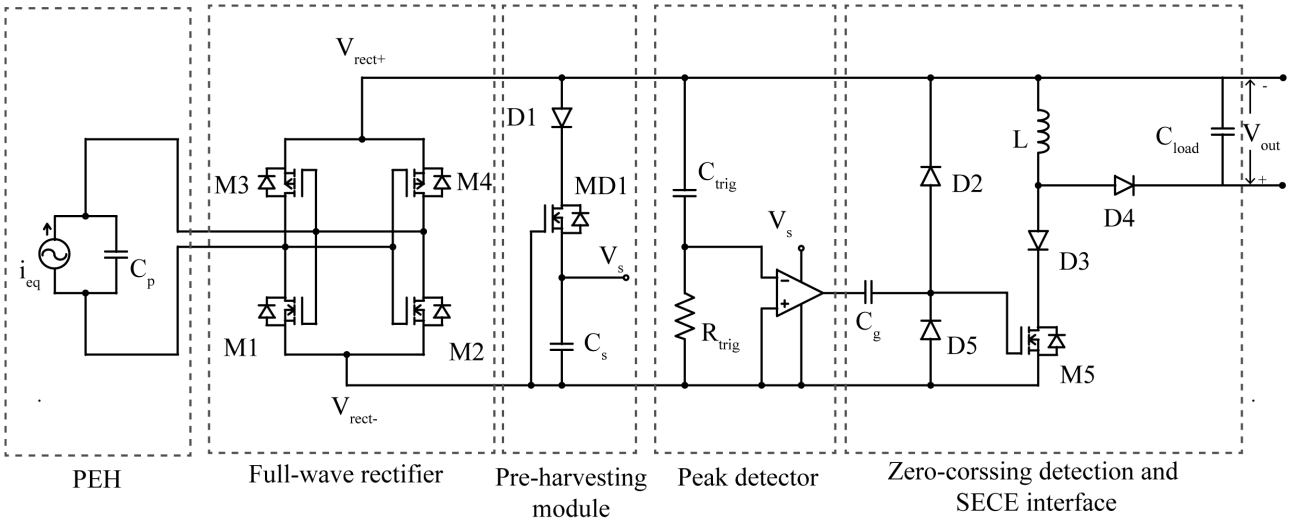

Fig. 1. Overview of proposed interface circuit.

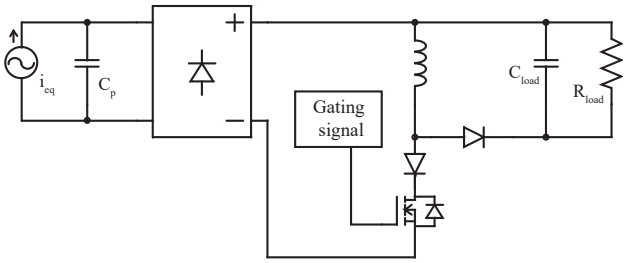

Fig. 2. SECE interface circuit

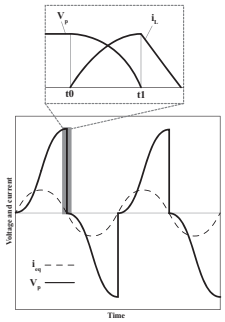

Fig. 3. Voltage and current waveform of SECE circuit

B. Pre-harvesting Circuit

Fig. 5(a) shows the schematic of pre-harvesting circuit. MD1 is a depletion MOSFET. The threshold voltage V_{th} of MD1 is negative, so MD1 will remain on as long as the voltage across C_s does not exceed $|V_{th}|$. When there's enough voltage on C_s, MD1 will turn off. Hence the output voltage V_s is given by (1).

$$V_s = \begin{cases} \max(V_{rect}) & \max(V_{rect}) \leq |V_{th}| \\ |V_{th}| & \max(V_{rect}) > |V_{th}| \end{cases} \quad (1)$$

Pre-harvesting circuit is connected behind the rectifier to harvest a small portion of the energy to supply power to the peak detector. The peak output voltage of rectifier is half of the peak-to-peak voltage, it and can be higher than 40 V in some cases. Such high voltage can damage the components in peak detection circuit, so MD1 is added for protection. Other protection method such as parallel connected zener diode will consume large amount of energy when V_s rises above the maximum voltage. The power consumption of this protection scheme is also less than those source-follower-like topology where a zener diode and resistor is connected in series to generate voltage reference.

With proper selection of V_{th}, the circuit can start working as soon as enough energy is delivered. If the minimum operational voltage of peak detector is higher than all the depletion type MOSFETs available, the protection topology can also be cascoded to output higher voltage. Fig. 5(b) shows a cascoded protection that has a maximum output voltage of $2|V_{th}|$, and more stage is possible.

In the cascoded configuration, the parallel connected resistor and capacitor serve to stablize the voltage at the gate terminal of MD2. Since the leakage current of MD1 will slowly charge the gate terminal and eventually make V_s reach max(V_{rect}), a large resistor is used to slowly discharge C_{GS} and C_1. The gate capacitance C_{gs2} is comparable to C_{DS1}, the drain-to-souce capacitance of MD1, this will affect the voltage level, so a capacitor that is much larger than C_{DS1} is added to make C_{DS1} neglectable.

Since the power is directly drawn from the PEH instead of the output, the pre-harvesting circuit also grants the ability of cold-starting-up. It can power the peak detector without any additional cold-start circuit, no pre charged battery or capacitor is required.

C. Peak Detector

Fig. 6 shows the schematic of the peak detector. C_{trig} and R_{trig} together forms a RC delay network. The voltage of the PEH is compared with a delayed version

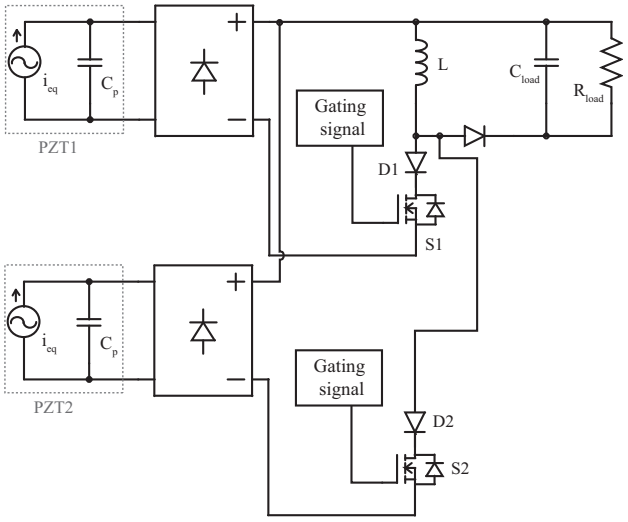

Fig. 4. SECE circuit for PEH array with two PEHs

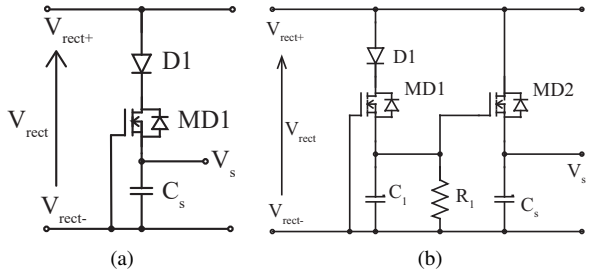

Fig. 5. Pre-harvesting circuit. (a) One stage pre-harvesting circuit. (b) Cascoded pre-harvesting circuit.

of itself so that the slope of the voltage is determined. The comparator generates a square wave $V_{trig}(t)$ where a rising edge corresponds to a voltage peak of the piezoelectric transducer.

The operational frequency range of such a peak detector is limited. When the frequency is too low, the voltage difference on R_{trig} would be smaller than the hysteresis of the comparator. When the frequency is too high, the detection delay is too large. But this bandwidth is still much larger than that of most mechanical structures used in piezoelectric energy harvesters. The design margin is enough for most cases. Thanks to the large input resistance of comparators, R_{trig} can be selected to be relatively large and C_{trig} can be small to decrease the power dissipation on R_{trig}.

D. Passive zero crossing detection

Fig. 7(a) shows the topology of SECE interface with zero crossing detection. The square wave control signal from peak detector is coupled to the gate of M3 through C_g. Fig. 7(b) shows the waveforms of V_{trig}, V_{rect} and the gate source voltage V_{gs} of M5 at a voltage peak of the PEH. t_0 indicates the arrival of the voltage peak. At t_0, a rising edge is sent from the peak detector to the gate of M5, the amplitude of which is slightly less than V_s. Since V_s must be smaller than the maximum voltage of V_{rect}, D2 will be reversely biased at this moment. As M5

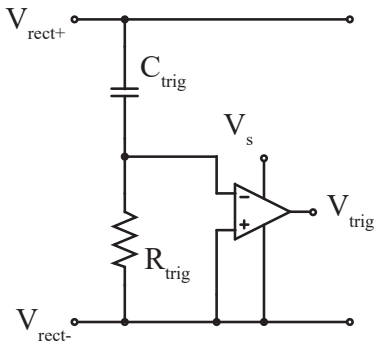

Fig. 6. Peak detector

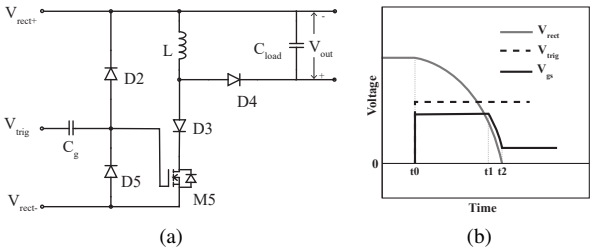

Fig. 7. Passive zero crossing detection and turning off. (a) schematic. (b). voltage waveform of V_{gs} of M5, V_{rect} and V_{trig}

turns on, the energy stored in the PEH is transferred to the load and V_{rect} begins to drop. When V_{rect} drops to be lower than V_s at t_1, D2 becomes forwardly biased and force V_{gs} to drop to V_{rect}. M5 becomes diode connected and remains on until $V_{rec} - V_{D2}$ falls below the threshold voltage of M5 at t_2, then M5 will turn off. By adjusting the threshold voltage of D2 or using multiple diodes in series, the turn off voltage can be adjusted. When V_{trig} becomes low again, C_g will discharge through D5, and one switch cycle completes.

The absolute value of turn-off voltage is not critical. It only needs to be less than the threshold voltage of the rectifier to avoid additional losses, as the rectifier will be cut off when PEH voltage drops below threshold value. Therefore no more energy can be harvested. D5 and D2 will be forwardly biased if V_{rect} becomes negative. So a rectifier is needed to keep V_{rect} positive.

E. Effect of Incomplete Charge Extraction

Threshold voltage of rectifiers and peak detector delay will cause incomplete charge extraction, as shown in Fig. 8. For peak detectors based on envelope detection, the detection delay will cause a fixed voltage loss, i.e., the charge extraction process will start after the voltage of PEH drops below peak voltage by a certain value. On the other hand, the threshold voltage of rectifier will cause some charges to be left in the PEH after extraction. In that case the charge extraction process will stop when the voltage of PEH drops below a certain value. The amount of output energy at each extraction is given by (2).

$$E_{\text{extracted}} = \frac{1}{2} C_p [(V_{ppoc} - V_H)^2 - V_L^2] \qquad (2)$$

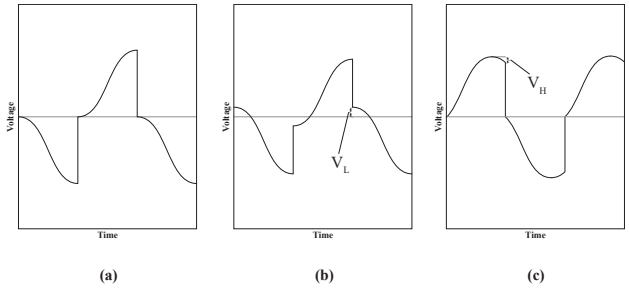

Fig. 8. Incomplete Charge Extraction.(a) Ideal SECE waveform with no incomplete charge extraction. (b) Incomplete charge extraction due to residual charge. (c) Incomplete charge extraction due to peak detection delay

TABLE I. COMPONENTS USED IN PROTOTYPE

Component	Part Number	Important Parameters
M1,M3	AO3415	V_{th} = 0.7V $V_{GS} = \pm 8V$
M2,M4	AO3414	V_{th} = 0.7V $V_{GS} = \pm 8V$
M5	ZVN4424GTA	V_{th} = 1.4V C_{GS} = 200pF
MD1	BSS159N	V_{th} = -2.4V
C_s	-	$C_s = 5\mu F$
C_{trig}	-	$C_{trig} = 1.5nF$
C_g	-	$C_g = 820pF$
D1,D4	BAT54	VF=0.24V @ 0.1mA IR=2 μA@25V
D2,D3,D5	1N4148	VF = 0.62V @ 5mA IR = 3 μA@20V
L	-	L = 120 mH ESR = 166 Ω@3 kHz

Where V_{ppoc} is open-circuit peak-to-peak voltage of PEH in deal case, V_H is the voltage loss caused by peak detector delay, and V_L is the voltage of the PEH after extraction. For a commonly used self-powered switch shown in Fig 9, $V_L = 0$ and $V_H = V_D + V_{BE}$. For the proposed circuit, $V_H = 0$ and $V_L = 2V_D$. If V_H and V_L is roughly the same, then for one energy extraction, (3) can be derived.

$$\frac{1}{2}C_p[(V_{ppoc}-V_H)^2-0^2] < \frac{1}{2}C_p[(V_{ppoc}-0)^2-V_L^2] \quad (3)$$

That is, if one of V_H and V_L has to be introduced into the harvesting system, and $V_H \approx V_L$, then introducing V_H will cause less power loss. This is how precise peak detection can help improve efficiency, even at the cost of leaving some residual charge in the PEH after charge extraction.

III. EXPERIMENTS

A. Experimental Setup

To evaluate the performance of ZSECE, a prototype is fabricated with discrete components and printed circuit board (PCB). Table I shows the parameters of the components used on the prototype. To reduce the effect of threshold voltage, The MOSFETs on the bridge rectifier have low threshold voltage at the cost of low breakdown voltage between gate and source and high C_{GS}. While M5 serves as a switch, so a MOSFET with low R_{DSON} and low C_{GS} is selected to reduce the driving loss and conduction loss.

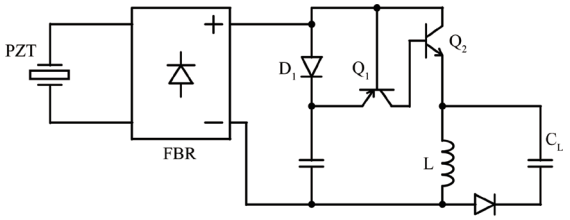

Fig. 9. Conventional self-powered SECE interface circuit based on peak detection [13]

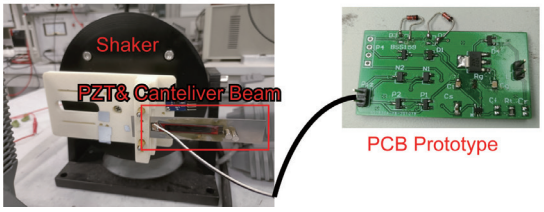

Fig. 10. Shaker, cantilever beam and PCB prototype used in experiments. The inductor is externally connected.

To compare the performance of ZSECE and other interface circuits, the self-powered SECE interface circuit in Fig. 9 is also fabricated with 1N4148, 2N3904 and 2N3906. And a full-wave rectifier is fabricated with 1N4148. All three interface circuits use the same type of output capacitor. And the two SECE circuits use the same L, D4, and C_{load} for fair comparison.

The PEH is attached to a vibration shaker powered by a power amplifier. A function generator provides a sinusoidal control signal of the power amplifier. The open circuit peak-to-peak voltage V_{pp} is adjusted manually before experiments. Fig. 10 shows the mechanical structure and PCB prototype.

B. Experimental Results

Fig. 11 shows the output power of a single ZSECE unit, a full-wave rectifier (SEH) and a conventional self-powered SECE circuit. The open circuit V_{pp} in this case is 12.0 V and frequency is 43.33 Hz. The output power drops slightly at high V_{out} because some current will leak through the drain of M5 in the harvesting process if V_{out} rises too high. ZSECE can harvest 79.3% more energy than SEH and 64.7% more energy compared to conventional self-powered SECE.

Fig. 12 shows the captured waveform of two ZSECE harvesting power from two different PEHs. The two ZSECE units share the same inductor and load. The load is 5MΩ. The red line and blue line are PEH voltage waveforms of 42 Hz and 35.9 Hz separately. The green line is ac coupled output voltage. At each voltage peak of PEH, the output voltage rises, indicating energy is transferred from PEH to load as expected. The output power of PEH1 (red line) alone is 46.39 μW. The output power of PEH2 (blue line) alone is 41.76 μW. The output

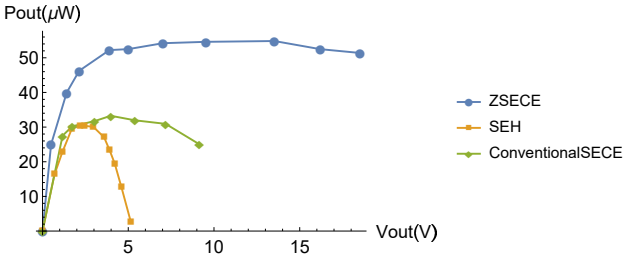

Fig. 11. Output power of ZSECE, Full bridge rectifier (SEH) and conventional self-powered SECE in Fig. 9

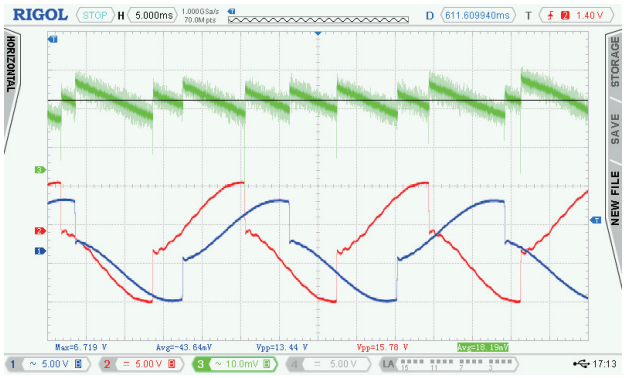

Fig. 12. Voltage waveform of two PEHs (red and blue) and output voltage (green)

power when both PEHs work simultaneously is 84.872 μW. The output power of both PEHs working together is slightly less than the sum of two PEHs working independently, since the output voltage is high.

IV. Conclusion

This paper introduced a self-powered SECE interface circuit with passive zero crossing detection (ZSECE) for piezoelectric transducer array energy harvesting. ZSECE can harvest energy from multiple PEHs with only one inductor regardless of their phase difference. Output power is almost load independent. It uses passive zero crossing detection to reduce cost. ZSECE can harvest 79.3% more energy compared to SEH and 64.7% more energy compared to self-powered SECE.

References

[1] J. Liang and W.-H. Liao, "Improved design and analysis of self-powered synchronized switch interface circuit for piezoelectric energy harvesting systems," IEEE Transactions on Industrial Electronics, vol. 59.

[2] D. Guyomar, A. Badel, E. Lefeuvre, and C. Richard, "Toward energy harvesting using active materials and conversion improvement by nonlinear processing," IEEE Transactions on Ultrasonics, Ferroelectrics, and Frequency Control, vol. 52, no. 4, pp. 584–595, 2005.

[3] E. Lefeuvre, A. Badel, C. Richard, and D. Guyomar, "Piezoelectric energy harvesting device optimization by synchronous electric charge extraction," Journal of Intelligent Material Systems and Structures, vol. 16, no. 10, pp. 865–876, 2005.

[4] A. Shareef, W. L. Goh, S. Narasimalu, and Y. Gao, "A rectifierless ac–dc interface circuit for ambient energy harvesting from low-voltage piezoelectric transducer array," IEEE Transactions on Power Electronics, vol. 34, no. 2, pp. 1446–1457, 2018.

[5] D. Koyama and K. Nakamura, "Array configurations for higher power generation in piezoelectric energy harvesting," in 2009 IEEE International Ultrasonics Symposium, pp. 1973–1976, 2009.

[6] Z. Chen, J. He, and G. Wang, "Vibration bandgaps of piezoelectric metamaterial plate with local resonators for vibration energy harvesting," Shock and Vibration, vol. 2019, 2019.

[7] L. Wang, T. Tan, Z. Yan, D. Li, B. Zhang, and Z. Yan, "Integration of tapered beam and four direct-current circuits for enhanced energy harvesting from transverse galloping," IEEE/ASME Transactions on Mechatronics, vol. 24, no. 5, pp. 2248–2260, 2019.

[8] X. Cui, M. Teng, and J. Hu, "Pspice-based analyses of the vibration energy harvester system with multiple piezoelectric units," Canadian journal of electrical and computer engineering, vol. 38, no. 3, pp. 246– 250, 2015.

[9] B. Y. Jing and K. S. Leong, "Demonstration of piezoelectric cantilever arrays for broadband vibration harvesting," in 2016 IEEE International Conference on Power and Energy (PECon), pp. 814–817. IEEE, 2016.

[10] Y. Li, X. Wang and Y. Xia, "Extensible piezoelectric energy harvesting circuit based on synchronous electric charge extraction with single inductor," 2019 IEEE International Conference on Electron Devices and Solid-State Circuits (EDSSC), 2019, pp. 1-3.

[11] D. Guyomar, G. Sebald, S. Pruvost, M. Lallart, A. Khodayari, and C. Richard, "Energy harvesting from ambient vibrations and heat," Journal of Intelligent Material Systems and Structures - J INTEL MAT SYST STRUCT, vol. 20.

[12] X. Wang, Y. Xia, G. Shi, H. Xia, Y. Ye, and Z. Chen, "Extensible multi-input synchronous electronic charge extraction circuit based on triple stack resonance for piezoelectric and thermoelectric energy harvesting," IEEE Transactions on Industrial Electronics.

[13] M. Lallart and D. Guyomar, "An optimized self-powered switching circuit for non-linear energy harvesting with low voltage output," Smart Mater. Struct., vol. 17, no. 3, p. 035030 (8pp), 2008